

Characterization of Coal and Biomass Conversion Behaviors in Advanced Energy Systems

Investigators

Reginald E. Mitchell, Associate Professor, Mechanical Engineering; Paul A. Campbell and Liqiang Ma, Graduate Researchers; Ilkka Saarenpää, Visiting Scholar

Introduction

The goal of this project is to develop models that predict accurately coal and biomass gasification and combustion behaviors in the type of environments likely to be established in advanced energy systems. This requires acquiring the information needed to understand and characterize the fundamental chemical and physical processes that govern coal and biomass conversion at high temperatures and pressures. The models can be used to determine operating conditions that optimize thermal efficiency and to examine design strategies for integrating combined cycles for the production of synthesis gas and electric power with minimum impact on the environment.

Background

The coal-fired power plant will continue to be the workhorse of America's electric power sector for the next 50 years. Improvements in burner designs, refractory materials and high-temperature heat exchangers in combination with hybrid schemes that combine coal combustion and coal gasification have the potential for the development of highly efficient, environmentally clean, power-generating technologies. The increased efficiencies yield lower emissions of greenhouse gases, carbon dioxide emissions being the most critical to reduce. Higher efficiencies also mean that less fuel is used to generate the rated power, resulting in improved system economics.

Biomass is a renewable fuel, and is considered to be CO₂-neutral with respect to the greenhouse gas balance if the use of fossil fuels in harvesting and transporting the biomass is not considered. By increasing the fraction of renewable energy in the energy supply, the extent that carbon dioxide emissions will adversely impact the environment can be diminished. Co-firing biomass with coal in traditional coal-fired boilers and furnaces or using biomass-derived gas as a reburn fuel in coal-fired systems represent two options for combined renewable and fossil energy utilization.

Configurations that employ both biomass and coal in integrated gasification combined gas and steam power cycles and hybrid technologies that produce synthesis gas for fuel cells as well as produce electric power in combined gas and steam power cycles offer additional options. Coal and biomass contain significant quantities of hydrogen, and several schemes have been advanced for the efficient and economical production of hydrogen from coal and biomass. With CO₂ capture and sequestration, partial coal or biomass oxidation is a promising technology for the production of electric power and hydrogen that uses integrated gasification combined-cycle technology with little adverse environmental impact.

The design of efficient coal/biomass co-utilization energy systems with integrated thermal management to minimize waste heat requires an understanding of the processes

that control the physical transformations that coal and biomass particles undergo when exposed to hot environments and the chemical reactions responsible for conversion of the solid material to gaseous species and ash. The design of efficient systems for the production of hydrogen from coal and biomass also requires an understanding of these physical and chemical processes. The goal of this research project is to provide the needed understanding. Our efforts will result in fundamentals-based sub-models for particle mass loss, size, apparent density, and specific surface area evolution during conversion of coal and biomass materials to gas-phase species during gasification and combustion processes.

During this third year of the project, we have (i) developed a model of a burning carbon particle that enabled us to characterize how the size and apparent density of char particles vary with mass loss during oxidation at high temperatures; (ii) validated our heterogeneous reaction mechanism at elevated pressures; (iii) constructed a high-pressure reaction chamber that will permit us to perform high-pressure combustion and gasification experiments under high heating rate conditions, conditions typical of industrial devices; and (iv) made reactivity measurements at elevated oxygen levels. An overview of the activities associated with these research areas follows.

Results

Characterization of Char-Particle Burning Behavior

Several studies have shown that during the combustion of coal particles in conditions typical of those existing in industrial, pulverized coal-fired boilers and furnaces, char particles burn in what is referred to as the Zone II burning regime, the regime in which particle burning rates are limited by the combined effects of chemical reaction and pore diffusion. Due to the oxygen concentration gradients established inside particles and the associated distribution of rates of mass loss due to chemical reaction, particle diameters, apparent densities, and specific surface areas decrease with mass loss when burning is in this regime.

In the Zone I burning regime in which oxidation occurs at low temperatures, rendering mass loss rates limited by chemical reaction rates, a particle burns more or less uniformly throughout its volume. Its size is relatively unchanged and its apparent density varies directly with mass loss. The specific surface area of the particle can be predicted using the grain and pore models that have been developed for such uniform burning. In the Zone III burning regime in which oxidation occurs at high temperatures, rendering mass loss rates limited by the rates of oxygen diffusion to the outer surfaces of particles, a particle burns primarily at its periphery. Its apparent density is relatively unchanged and its diameter varies to the 3rd power with mass loss. The specific surface area of the particle is relatively unchanged in this burning regime, there being relatively little interior burning during mass loss.

In the Zone II burning regime, the variations in particle size, apparent density, and specific surface area with mass loss have not been characterized to the extent that these particle properties can be predicted based on the extent of conversion. The power-law mode of burning model ($\rho_C/\rho_{C0} = (m_C/m_{C0})^\alpha$; $D_p/D_{p0} = (m_C/m_{C0})^\beta$, with $\alpha + 3\beta = 1$ for spherical particles), which is commonly used to predict apparent density and size

variations with mass loss during Zone II burning, assumes that the burning mode during the early stages of burning is the same as that during the late stages, and becomes inaccurate late in burnoff when burning shifts to the zone I regime before complete burnout. Development of a mode of burning model that is valid throughout the lifetime of a burning char particle is one of the goals of this research project.

Theoretical Development: In the theoretical approach taken, a spherical char particle initially of size D_{p0} , apparent density ρ_{C0} , and specific surface area S_{gC0} , is divided into K concentric annular volume elements, V_k , each of which contains a portion of the initial total mass of the particle ($m_{C0,k} = \rho_{C0}V_k$) that burns at a rate governed by the local conditions. The rate that the mass of the carbonaceous particle material in each volume element is oxidized is governed by the equation

$$\frac{1}{m_{C,k}} \frac{dm_{C,k}}{dt} = R_{iC,k} S_{gC,k} , \quad (1)$$

where the intrinsic chemical reactivity of the particle material depends upon the local oxygen concentration, which is governed by the following equation:

$$\frac{\partial C_{O_2}}{\partial t} - \frac{1}{r^2} \frac{d}{dr} \left(r^2 D_{eff} \frac{\partial C_{O_2}}{\partial r} \right) = -\hat{R}_{iO_2} \rho_C S_{gC} = -R_{iC} \nu_{O_2} \rho_C S_{gC} / \hat{M}_C . \quad (2)$$

When evaluating D_{eff} , account is made for the combined effects of bulk and Knudsen diffusion of oxygen through pores, surface roughness, the local porosity, and the particle tortuosity.

Simultaneous integration of Eqs. (1) and (2) yields the state of the particle at various times during its lifetime. The conversion and apparent density in each volume element are determined from the relations

$$x_{C,k} = 1 - m_{C,k} / m_{C0,k} \quad \text{and} \quad \rho_{C,k} = m_{C,k} / V_k , \quad (3a,b)$$

and the specific surface area of the carbonaceous material in volume element k is calculated using the expression

$$S_{gC,k} = S_{gC0,k} (1 - x_{C,k}) \left(\frac{\rho_{C0,k}}{\rho_{C,k}} \right) \sqrt{1 - \psi \ln(1 - x_{C,k})} . \quad (4)$$

This expression for the specific surface area, due to Bhatia and Perlmutter [1], accounts for the opposing effects of pore growth and pore coalescence during char conversion under Zone I burning conditions. The relative competition between area formation and area destruction is controlled by the value of the structural parameter ψ . The mass, apparent density and specific surface area of the char particle at any instant are calculated using the relations

$$m_C = \sum_k m_{C,k} , \quad \rho_C = m_C / \sum_k V_k , \quad \text{and} \quad S_{gC} = \sum_k (S_{gC,k} m_{C,k}) / m_C . \quad (5a,b,c)$$

An overall oxygen conservation equation provides the link between the oxygen partial pressure in the gas phase surrounding the particle and that at the outer surface of

the particle. Equating the flux of oxygen at the outer surface of the particle to the overall consumption rate of oxygen inside the particle yields the following set of relations for the overall particle burning rate per unit external surface area:

$$q = \frac{k_d P}{\gamma} \ln \left(\frac{1 - \gamma P_s / P}{1 - \gamma P_g / P} \right) = \left(1 + \frac{\eta D_p \rho_C S_{gC}}{6} \right) R_{iC,ex} \quad (6a,b)$$

The effectiveness factor η , which accounts for the oxygen reactivity distribution inside the particle, is calculated from the oxygen consumption rate in each of the volume elements into which the particle is divided, as follows:

$$\eta = \frac{\sum_k \hat{R}_{iO_2,k} \rho_{C,k} S_{gC,k} V_k}{\sum_k \hat{R}_{iO_2,max} \rho_{C,k} S_{gC,k} V_k} = \frac{\sum_k \hat{R}_{iO_2,k} \rho_{C,k} S_{gC,k} V_k}{\sum_k \hat{R}_{iO_2,ex} \rho_{C,k} S_{gC,k} V_k} \quad (7)$$

The maximum reactivity of oxygen presumably occurs at the particle external surface, where the oxygen concentration is highest.

Char-particle temperature is calculated from the following energy balance, wherein the rates of energy generation due to char oxidation are balanced by the rates of energy loss by conduction, convection, and radiation:

$$q \Delta H = - \frac{Nu \lambda}{D_p} \frac{\kappa}{1 - e^\kappa} (T_p - T_g) + \varepsilon \sigma (T_p^4 - T_w^4), \quad \text{where} \quad \kappa = \frac{\gamma c_{p,g} D_p \nu_{O_2} q}{\hat{M}_C \lambda Nu} \quad (8)$$

In this equation, q denotes the overall particle burning rate per unit external surface area and T_g , T_p , and T_w denote the temperatures of the gas, particle and walls to which particles radiate, respectively.

The intrinsic chemical reactivity of the carbonaceous material is determined from the heterogeneous reaction mechanism shown in Table I. In the reactions, C_f represents a free carbon site, one available for oxygen chemisorption, and $C(O)$ represents a carbon site filled with a chemisorbed O atom. The mechanism is based on the carbon reactivity model developed by Haynes [2]. Hurt and Calo [3] have shown that this type mechanism is capable of describing the trends reported in various studies with respect to reaction order, activation energy, and CO-to-CO₂ product ratio.

Table I. Heterogeneous reaction mechanism

Chemical reaction	A*	E (kJ/mol)
(R1) $2 C_f + O_2 \rightarrow CO + C(O)$	1.39×10^5	66.0
(R2) $C_f + C(O) + O_2 \rightarrow CO_2 + C(O) + C_f$	5.03×10^{10}	137.0
(R3) $C_f + C(O) + O_2 \rightarrow CO + C(O) + C(O)$	7.96×10^{15}	236.0
(R4) $C(O) \rightarrow CO + C_f$	3.58×10^{10}	236.0

* units consistent with surface concentrations in mol/m²-surface, gas concentrations in mol/m³-fluid, and time in s.

$$RR_i = k_i \prod_j [X_j]^{v_j}; \quad k_i = A_i \exp(-E_i / \hat{R}T); \quad [X_j] = \text{concentration species } j$$

The Arrhenius parameters shown in the table are based on results of our previous work on the reactivity of the char of a bituminous coal (Lower Kittanning) for which $\rho_{C0} = 0.49 \text{ g/cm}^3$, $S_{gC0} = 143 \text{ m}^2/\text{g}$, and $\psi = 2.8$ [4]. With this mechanism, the intrinsic char reactivity and adsorbed oxygen atom site fraction (θ_O) are given by

$$R_{iC} = \hat{M}_C (RR_1 + RR_2 + RR_3 + RR_4) \quad \text{and} \quad \frac{d\theta_O}{dt} = (N_{AV}/S)(RR_1 + RR_3 - RR_4) \quad (9a,b)$$

where RR_i is the overall reaction rate for reaction i . Equation (9a) is used in Eqs. (1) and (2) and Eq. (9b) is integrated simultaneously with Eqs. (1) and (2).

Calculated Results: In the calculations discussed below to demonstrate the capability of our model, the initial char particle radius ($D_{p0} = 100 \mu\text{m}$) was divided into 103 increments, distributed such that the initial mass in each of the 103 volume elements into which the overall particle volume was partitioned, was nearly the same. The non-uniform radial grid was used in the finite difference representation of Eq. (2). The resulting system of 309 ordinary differential equations were integrated simultaneously for the mass, oxygen concentration, and adsorbed oxygen atom concentration (site fraction) in each volume element for specified integration times up through 99% overall char conversion.

Shown as symbols in Fig. 1 are calculated size, apparent density and specific surface area profiles as functions of conversion for burning under conditions that render burning in Zones I and II during the course of mass loss. In each of the environments, at very early times when the adsorbed oxygen atom concentrations are low, modest amounts of oxygen penetrate the particle. Initially, burning is in Zone I at both low and high temperatures.

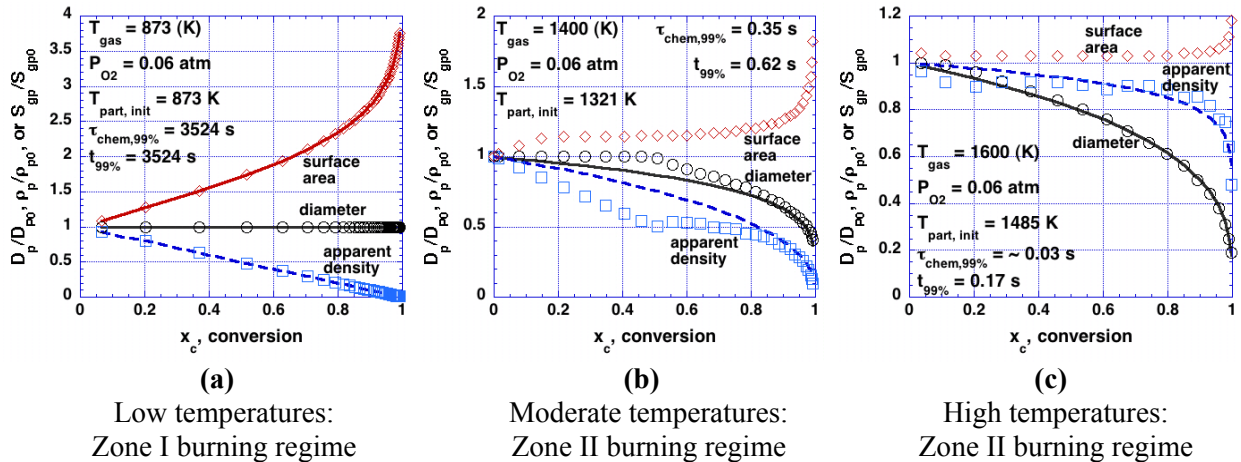


Figure 1: Calculated size, apparent density and specific surface area profiles during oxidation in selected environments.

The profiles shown in Fig. 1a exemplify Zone I burning: diffusion is fast compared to chemical reaction; the oxygen concentration is relatively uniform throughout the particle. The solid and dashed lines were calculated using the power-law mode of burning model with $\alpha = 1$, for constant diameter burning. The line for specific surface area was

calculated using Eq. (4), assuming uniform internal burning with $\psi = 2.8$, a typical value for coal chars.

At moderate gas temperatures (Fig. 1b), there is significant internal burning up until about 50% conversion. Up to this point, burning is close to the Zone I burning regime boundary, as evidenced by the constant diameter burning. The surface area, however, does not show the increase indicative of oxidation in the Zone I burning regime. Once the oxygen that penetrated the particle at early times is consumed, the particle burns primarily at its periphery until about 80% conversion, at which point the particle burns with significant decreases in both size and apparent density. The solid and dashed lines in Fig. 1b were calculated using the power-law mode of burning model with $\alpha = 0.4$, which provides adequate characterization of size and apparent density changes with mass loss at conversions greater than 80% but not less. No value of ψ in Eq. (4) yields the type variation in surface area with conversion shown in the figure.

At high temperatures (Fig. 1c), after the consumption of the oxygen that penetrated the particle at early times (which modestly reduced the apparent density), burning is confined to the particle periphery. Apparent density is nearly constant up to about 90% mass loss. The solid and dashed lines were calculated using the power-law mode of burning model with $\alpha = 0.1$, which provides adequate characterization of size and apparent density changes with mass loss over the entire conversion range, although at low conversions, diameter reductions are slightly under-predicted and apparent density reductions are slightly over-predicted. Again, Eq. (4) cannot yield calculated variations in specific surface area that agree with the trend shown in Fig. 1c, with any value of the surface area parameter ψ .

Of particular interest is the prediction of the particle's effectiveness factor during conversion under conditions when the burning rate is limited by the combined effects of pore diffusion and the intrinsic chemical reactivity of the particle material. Results are shown in Fig. 2, where the effectiveness factor is given as a function of the Thiele modulus, ϕ . The $\phi-\eta$ relation is described adequately using the relation

$$\eta = \frac{3}{\phi_m} \left(\frac{1}{\tanh \phi_m} - \frac{1}{\phi_m} \right)$$

where $\phi_m = \phi \sqrt{(m+1)/2}$ and $\phi = (D_p/2) \sqrt{R_{iO_2,ex} \rho_C S_{gC} / (C_{O_2,ex} D_{eff})}$

This $\phi-\eta$ relation is based on the reactivity being proportional to the first power of the oxygen concentration ($m = 1$). Using the modified Thiele modulus approach of Metha

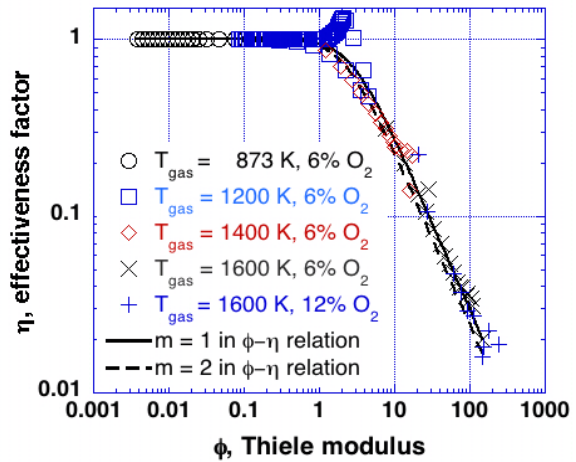


Figure 2: Effectiveness factor versus Thiele modulus.

and Aris [5], the reaction mechanism employed exhibits an overall reaction order between one and two with respect to the oxygen concentration, C_{O_2} . Note that in the 1200 K, 6% O_2 environment, effectiveness factors can exceed unity (at early times), a consequence of the adsorbed oxygen atom concentration being higher on internal surfaces than on the external surface of the particle, due to the oxygen that penetrated the particle at early times.

Based on the predictions of the above model, we are developing a specific surface area sub-model that is adequate for burning under zone II burning conditions. Model results are also being used to help develop a mode of burning sub-model that permits the prediction of particle size and apparent density from its mass based on the instantaneous state of the particle. The $\phi-\eta$ relation derived above will be employed to characterize the impact of partial oxygen penetration inside the particle owing to diffusional effects. These sub-models can be used with robust furnace models that take into account gas-phase reactions and flow field dynamics as well as char oxidation.

Char Reactivity at Elevated Pressures

Technologies that utilize fossil fuels at elevated pressures, such as pressurized fluidized bed combustion and high-pressure coal gasification, have attracted increasing research interests. Pressurized gasification and combustion of fossil fuels have the advantages of increased conversion efficiency, decreased pollutant emissions, and reduced reactor furnace size [6]. The database on pressurized char reactivity to oxygen is rather limited; data are insufficient to answer some of the most rudimentary questions concerning the impact of pressure on coal reactivity. Some studies show a relatively small dependence of the rates of char oxidation on total pressure whereas other tests show a significant impact. Our efforts are directed at resolving this controversy. To this end, we have undertaken experiments to increase the data available on the conversion rates of coal chars at elevated pressures and to use the data to characterize the separate effects of total pressure and oxygen mole fraction on char reactivity.

In the initial phases of this study to characterize the impact of total pressure of char reactivity to oxygen, we have measured the intrinsic chemical reactivities of synthetic chars at selected pressures and oxygen concentrations at temperatures between 723 K and 873 K in our thermogravimetric analyzer. At these relatively low temperatures, the overall char mass loss rates in all the combustion tests were limited by chemical kinetics effects. We believe that part of the controversy that arises in the literature about the impact of pressure on char reactivity to oxygen stems from the fact that not all tests were performed under conditions in which chemical kinetics was rate-controlling. In some of the tests, mass transport effects were relatively significant, leading to erroneous conclusions about the impact of pressure on reactivity. Whereas chemical reaction rates increase with increasing pressure, rates of mass transport via molecular diffusion decrease with increasing pressure.

Experimental Procedure: A series of experiments using synthetic chars was performed. The use of synthetic char allows the study of char combustion without the possible catalytic effects of ash and without the complications of unknown chemical composition and unknown porosity inherent in real coals. The 16% porosity char that was used in the

study was synthesized using only carbon black as a pore-former and hence, had a microporous structure, with the largest pores being about 0.05 μm in diameter. The char was crushed and sieved to yield particles for testing in the size range 75 - 106 μm . The approximate and ultimate analyses of the char are shown in Table II.

Table II. Approximate and ultimate analyses of 16% porosity synthetic char

Approximate Analysis			Ultimate Analysis (daf)				
VM (wt%)	Fix-C (wt%)	Ash (wt%)	C (wt%)	H (wt%)	O ^a (wt%)	N (wt%)	S (wt%)
13.92	85.1	0.98	96.46	1.62	< 0.01	0.83	0.38

^a Obtained by mass balance

A pressurized thermogravimetric analyzer was used to obtain char conversion rate data and to make gas adsorption measurements for specific surface areas. The oxidation tests were performed at total pressures of 0.1, 0.2, 0.4, 0.8 MPa and oxygen mole percents of 3%, 6% and 12%, at temperatures low enough to ensure that mass loss rates were controlled solely by the intrinsic reactivity of the carbonaceous material and not limited by any mass transport effects. Conversion rates in the test environments were obtained by differentiating the measured weight loss profiles. The surface area measurements were made at room temperature and a pressure of 1 MPa, using CO₂ as the absorbing gas. The approach due to Brunauer, Emmett, and Teller [7] was used in the analysis of the adsorption data to yield specific surface areas.

Experimental Results: The results in Fig. 3 show that in the zone I burning regime, the specific surface area, measured *in situ* during the oxidation test, continuously increases until quite late in burnoff. The solid curve was calculated using the expression based on Eq. (4). The structural parameter ψ of value 7.0 was determined from a least-square fit to the *in situ* surface area data. According to Bhatia and Perlmutter [1], a ψ -value above 2.0 indicates that up to a conversion between about 30% and 50%, new surface area is exposed due to the opening of closed pores. A ψ -value between 0 and 2.0 indicates the char is not exposing any new surface areas during conversion. The data support the use of this specific surface area model for the zone I burning regime.

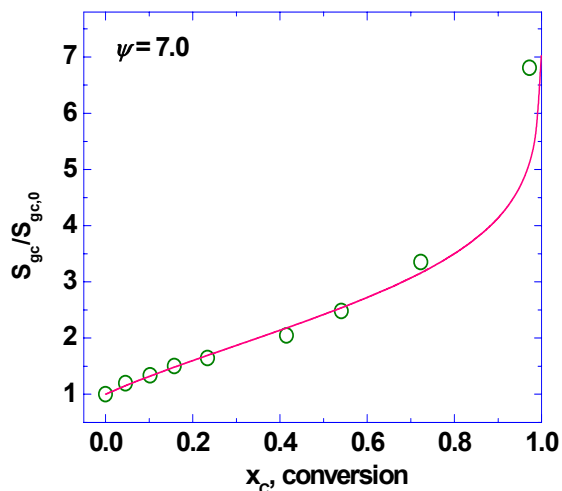


Figure 3: Surface area evolution in the zone I burning regime: $P = 0.4$ MPa and $T = 723$ K.

Shown in Figure 4 are char reactivities for different total pressures at a constant oxygen mole percent of 6%. These results indicate that the intrinsic reactivity increases with increasing total pressure at constant oxygen mole fraction.

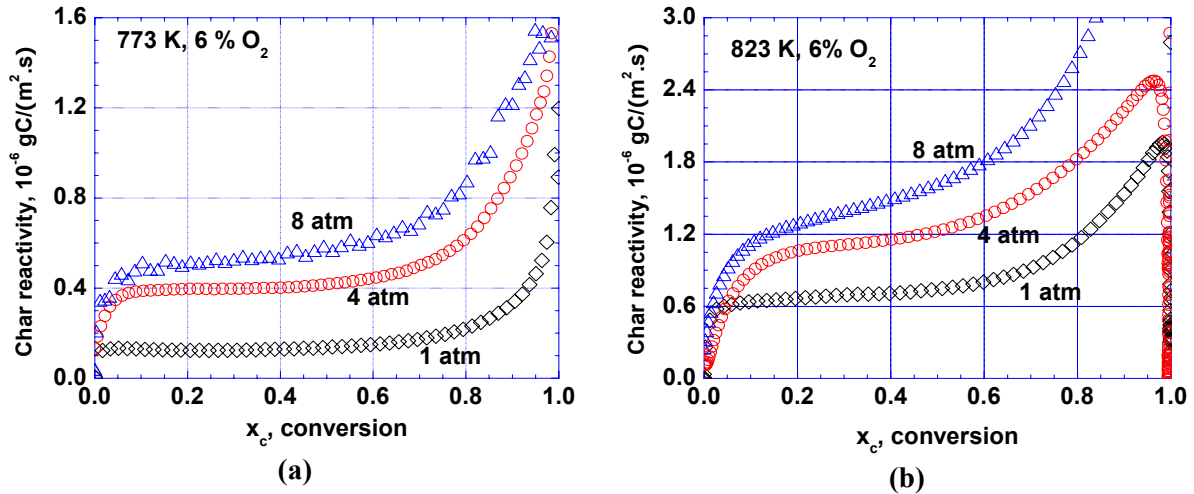


Figure 4: Char intrinsic reactivity vs. conversion at different total pressures ($P = 0.1, 0.4, \text{ and } 0.8 \text{ MPa}$) and constant oxygen mole fraction of 0.06.

Shown in Figure 5 is intrinsic reactivity as a function of conversion at a fixed total pressure of 0.8 MPa and oxygen mole percents from 3% to 12% at temperatures of 723 K and 773 K. At fixed temperature and total pressure, reactivity increases with increasing oxygen content. Combining this result with the result above, it is clear that the reactivity increases with increasing oxygen partial pressure, P_{O_2} . Comparison of the data in the left and right panels of Figs. 4 and 5 reveals that for a given oxygen level and total pressure, reactivity increases with increasing temperature, as expected.

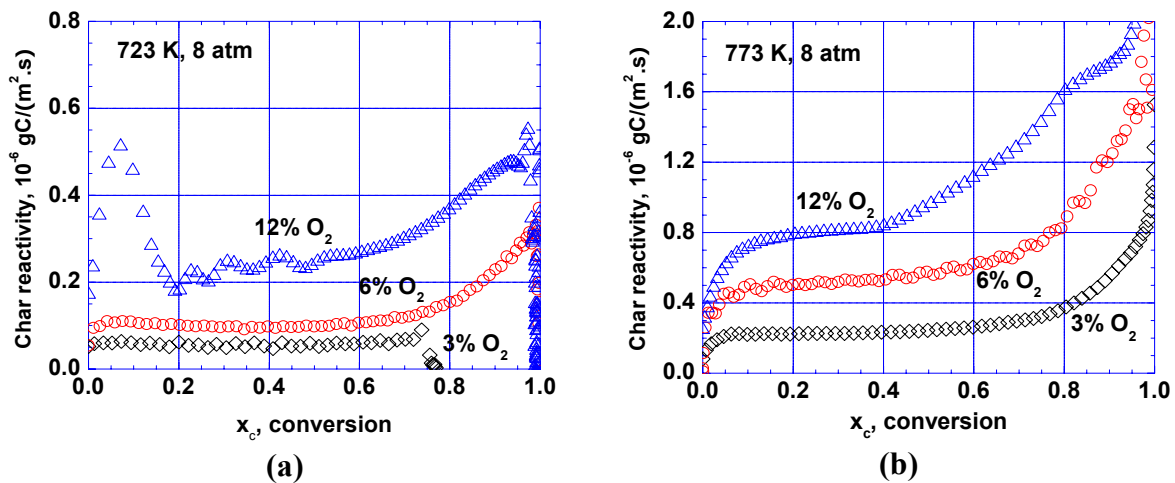


Figure 5: Char intrinsic reactivity as a function of conversion at selected oxygen mole fractions ($y_{O_2} = 0.03, 0.06 \text{ and } 0.12$) and constant total pressure ($P = 0.8 \text{ MPa}$).

The effect of total pressure on reactivity with constant oxygen partial pressure was also examined. The data are plotted in Fig. 6. For an oxygen partial pressure of 0.024 MPa and temperature of 773 K, as in the left panel of Fig. 6, the reactivities are almost the same over the entire range of conversion. The data shown in the right panel of Fig. 6, for an oxygen partial pressure of 0.048 MPa and temperature of 723 K, also

exhibit this behavior. Together with the above result that reactivity increases with increasing oxygen partial pressure, the data indicate that at a given temperature, the reactivity is solely determined by oxygen partial pressure ($P_{O_2} = y_{O_2} P$), independent of the individual values of total pressure P and oxygen mole fraction y_{O_2} .

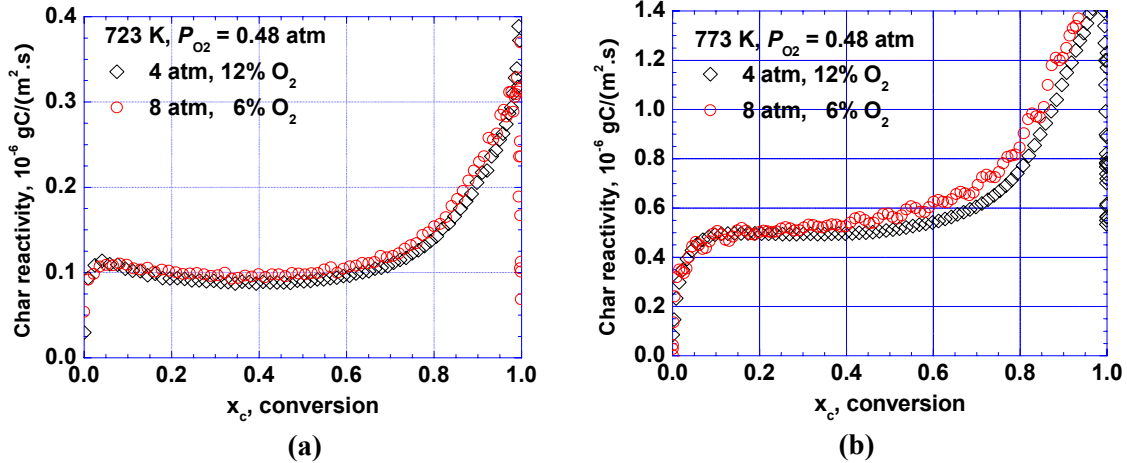


Figure 6: Effect of total pressures on reactivity at constant oxygen partial pressure ($P_{O_2} = 0.024$ and 0.048 MPa).

The data points in Figure 7 show the intrinsic reactivity profiles determined from experiments and the dashed curves show reactivity profiles calculated using the heterogeneous reaction mechanism discussed above. The profiles exhibit an initial rapid increase with conversion up to about 10% to 20% conversion followed by a slower increase before a relatively significant increase in the late stages of burning. This observation indicates that the adsorbed oxygen site fraction θ_O does not reach its quasi steady state value until relatively late in burnoff.

Table III shows values determined for the Arrhenius parameters for the reaction rate coefficients. The pre-exponential factor for the desorption reaction (reaction R4), was set to be within the range consistent with criteria suggested by Du *et al.* [8], resulting in an activation energy for desorption of 267 kJ/mol. This value is within the range expected for the desorption reaction [2, 8].

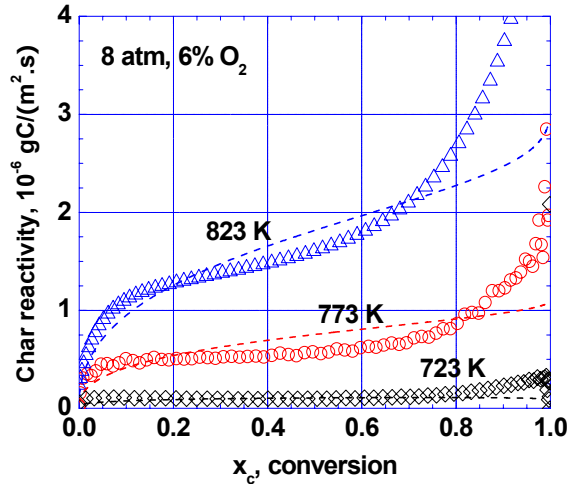


Figure 7: Measured and calculated intrinsic char reactivity vs. conversion at $P = 0.8$ MPa and $y_{O_2} = 0.06$.

Table III. Arrhenius Reaction Rate Parameters, $k = A \exp(-E/RT)$,
for a 16% Porosity Synthetic Char (see Table II for composition)

Chemical reaction	A*	E (kJ/mol)
(R1) $2 C_f + O_2 \rightarrow CO + C(O)$	2.61×10^2	44.6
(R2) $C_f + C(O) + O_2 \rightarrow CO_2 + C(O) + C_f$	5.15×10^{11}	166.2
(R3) $C_f + C(O) + O_2 \rightarrow CO + C(O) + C(O)$	1.88×10^{17}	275.9
(R4) $C(O) \rightarrow CO + C_f$	1.09×10^{12}	267.1

* units consistent with surface concentrations in mol/m^2 , gas concentrations in mol/m^3 -fluid, and time in s.

The agreement between measurements and calculations shown in Fig. 7 indicates that the reaction mechanism based on the model of Haynes [2] accurately characterizes char oxidation at elevated as well as atmospheric pressures when burning is under zone I burning conditions. Analyses of the data that we have amassed combined with calculations have led us to the conclusion that the transition temperature from the zone I to the zone II burning regime decreases with increasing total pressure. Whereas at 873 K and 0.1 MPa the synthetic pulverized coal char particles burn under kinetically-controlled conditions, at 873 K and 0.8 MPa, the char particles burn under conditions limited by the combined effects of chemical reaction and pore diffusion. At 0.8 MPa, char-particle burning is chemical kinetics-limited only at temperatures less than about 773 K.

High Pressure Reaction Chamber Construction

The char used in the above study to examine the impact of pressure of char reactivity was produced at atmospheric pressure in our tubular furnace. Consequently, the chars are not characteristic of the chars produced at elevated pressures under high heating rate conditions as they are in pressurized industrial furnaces and boilers. Pressure influences coal swelling and the yields of volatiles during devolatilization. Consequently, it influences the structure and morphology of the char generated. Pulverized coal char particles produced at high heating rates and high pressures have a morphology that is more cenospheric in character than chars produced at atmospheric pressure. Low to medium porosity particles having large voids inside their outer walls, both single-cavity and multiple-cavity and thin-walled and thick-walled, are produced at elevated pressures, the higher the pressure, the thinner the walls and the fewer the cavities. Because of these differences in char structure, in the same oxidation environment, a char produced at a high pressure will lose its mass at a faster rate than a char produced at a lower pressure.

Relatively few studies can be found in the literature that are concerned with characterizing the impact of char structure and morphology on char conversion rates. Pressures up to 50 atm are likely to be used in advanced pressurized fluidized bed combustors and coal-fired power plants that employ integrated gasification combined cycle technology. Fundamental understanding of the effects of operating pressure on coal reactions is essential to the development of these technologies. Our goal is to provide the understanding needed to develop models that predict accurately the impact of pressure on coal and biomass conversion phenomena.

Since the onset of this project, we have designed, fabricated, and constructed a pressurized chamber that will enclose the entrained flow reactor that we use in our high-

temperature oxidation tests. A flow control panel is almost complete. The pressurized facility will permit high-pressure oxidation tests up to 50 atm, permitting the investigation of the effects of pressure on coal conversion rates under conditions typical of high-pressure industrial furnaces and boilers. We anticipate shake-down tests by early summer with the actual testing of coals and biomass materials beginning by the end of the summer.

Char Reactivity at Elevated Oxygen Levels

One of our goals is to assess the extent to which the reactivity of a biomass char can be predicted based on its fractional contents of cellulose, hemicellulose and lignin, the principle constituents of biomass. This requires testing a variety of biomass materials and determining parameters that describe their reactivities. Since new technologies may employ oxygen-enhanced combustion, some of our tests have been performed under oxygen-enriched conditions. Increasing the oxygen content of the oxidizer enhances product throughput and efficiency, yields a flue gas having a relatively high CO₂ concentration, and reduces the carbon in ash. In addition, with advances in low-temperature oxy-fuel burner designs, reductions in the emissions of nitrogen oxides can also be realized with oxygen-enhanced combustion. Oxy-fuel combustion combined with CO₂ capture is a technology that can be applied to both new and existing pulverized coal-fired power plants to yield highly efficient, non-polluting energy conversion systems.

Figure 8 shows photographs taken of pulverized peat particles burning in our laminar flow reactor when the flow rates of the gases fired to the reactor (CH₄, H₂, O₂, and N₂) were adjusted to yield a reactor environment at nominally 1350 K with oxygen levels ranging from trace amounts to 48%, by volume, as indicated in the figure captions. The emission is almost entirely from combustion of the volatiles released during devolatilization when oxygen levels are less than 3%, by volume, at 1350 K. At higher oxygen levels, the emission is from radiating char particles as well. In the 24% and 48% oxygen environments, the burning char particles reach temperatures several hundred degrees higher than the gas temperature; char reaction rates are quite high. The bright luminous emission disappears comparatively early in the 48% oxygen environment; the char has almost completely burned out at the high reaction rates.

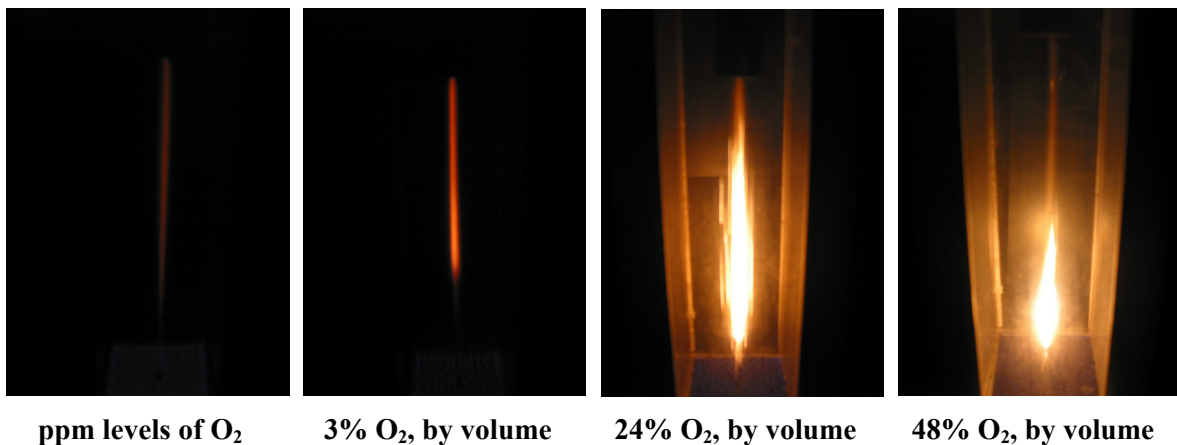


Figure 8: Photographs of pulverized biomass particles burning in the laminar flow reactor. Gas temperatures are nominally 1250 K.

In each of the environments, partially reacted chars were extracted from the flow reactor at successive extents of burnoff and analyzed to determine, amongst other properties, the char reactivity to oxygen. Although we have not yet completed analysis of the data amassed, preliminary data analysis indicate that in the 24% and 48% oxygen environments, char oxidation began before devolatilization was complete. This complicates analysis of the data to determine kinetic parameters for the oxidation reactions. Account has to be made for mass loss due to devolatilization before oxidation rates can be determined. Presently we are reviewing the literature, surveying models that have been developed for biomass devolatilization. We plan to select one and use data obtained in the environment containing trace amounts of oxygen to determine parameters in the devolatilization model selected. The model will then be used to predict the mass loss due to devolatilization in the higher oxygen level environments. In this way, mass loss due solely to heterogeneous char oxidation can be estimated, and used to determine kinetic parameters for the heterogeneous oxidation reactions.

Progress

Considerable progress has been made towards developing the understanding needed to predict accurately the behaviors of coal and biomass chars during conversion in high-temperature, high-pressure environments. At atmospheric pressures, we can predict quite accurately the manner in which the sizes, apparent densities and specific surface areas of char particles vary with mass loss under conditions in which mass loss rates are limited by the combined effects of pore diffusion and the intrinsic chemical reactivity of the particle material. The ability to make accurate predictions at elevated pressures is forthcoming; tests to characterize the impact of pressure on the reactivity of chars produced under high-pressure conditions still need to be performed.

The work being performed will allow us to characterize accurately the chemical and physical changes that coal and biomass particles undergo during combustion and gasification processes under conditions likely to occur in advanced energy conversion systems. The data obtained will permit the development and validation of the physical and chemical sub-models needed in comprehensive models for coal-fired and biomass-fired process units. The comprehensive models can be used to investigate potential design strategies and can help define optimum operating conditions that yield high coal and biomass conversion efficiencies with minimum impact on the environment.

Future Plans

Studies to determine the relationship between model parameters and coal and biomass properties are ongoing as are studies to characterize the impact of the ash-content of particles on char reactivity. Also ongoing are studies to assess the extent to which the reactivity of a biomass char can be predicted based on its fractional contents of cellulose, hemicellulose, and lignin. Data obtained with all the coal and biomass chars we examine are used in these efforts. We will continue to measure the reactivities of coal and biomass chars burning at elevated pressures in our pressurized thermogravimetric analyzer when burning is in the zone I burning regime. Once the high-pressure facility is completed, we will begin to characterize reactivity differences due to morphological changes that occur as a consequence of devolatilization at high pressures. The studies

undertaken will help us to understand how coal and biomass properties influence char conversion rates in high-temperature, high-pressure environments.

Publications

The following papers were presented at conferences during the past year:

1. Mitchell, R. E. "Characteristics of Pulverized Coal and Biomass Combustion," Invited Seminar, Chemical Engineering Department, Brigham Young University, February 10, 2005.
2. Mitchell, R. E. "Burning Behaviors of Pulverized Coal and Biomass Char Particles," Nineteenth Annual ACERC & ICES Conference, Brigham Young University, Provo, UT, February 17-18, 2005.
3. Ma, L. and Mitchell, R. E. "Char Reactivities to Oxygen at Elevated Pressures," presented at the Fourth Joint Meeting of the U.S. Sections of the Combustion Institute, Paper D31, Philadelphia, PA March 20-23, 2005.
4. Mitchell, R. E. and Ma, L. "On the Burning Behaviors of Coal and Biomass Chars," presented at the Fourth Joint Meeting of the U.S. Sections of the Combustion Institute, Poster P26, Philadelphia, PA March 20-23, 2005.

References

1. Bhatia, S. K., and Perlmutter, D. D., *AIChE Journal* 26: 379-386, (1980).
2. Haynes, B. S., *Combust. Flame* 126: 1421-1432 (2001).
3. Hurt, R. H. and Calo, J. M., *Combustion and Flame* 125:1138-1149 (2001).
4. Campbell, P. A., Mitchell, R. E., and Ma, L., *Proc. Combust. Inst.* 29: 2261-2270 (2002).
5. Mehta, B. N. and R. Aris, *Chemical Engineering Science*, 26, 1699 (1971).
6. Harris, D. J. and Patterson, J. H., *Aust. Inst. Energy J.*, 13:22 (1995).
7. Brunauer, S., The Adsorption of Gases and Vapours, Oxford University Press, Oxford, and Princeton University Press, Princeton, N.J. (1945).
8. Du, Z, Sarofim, A. F., and Longwell, J. P., *Energy and Fuels* 4:296 (1990).

Contact

Reginald E. Mitchell: remitche@stanford.edu